Translational Science

Cancer Research

miR-139-5p Modulates Radiotherapy Resistance in Breast Cancer by Repressing Multiple Gene Networks of DNA Repair and ROS Defense

Marina Pajic[1,2], Danielle Froio[1], Sheridan Daly[1], Louise Doculara[1], Ewan Millar[1,3,4], Peter H. Graham[1], Alison Drury[1], Angela Steinmann[1], Charles E. de Bock[5], Alice Boulghourjian[1], Anaiis Zaratzian[1], Susan Carroll[6], Joanne Toohey[6], Sandra A. O'Toole[1,7,8], Adrian L Harris[9], Francesca M. Buffa[9], Harriet E. Gee[1,6,8], Georgina E. Hollway[1,2], and Timothy J. Molloy[2,10]

Abstract

Radiotherapy is essential to the treatment of most solid tumors and acquired or innate resistance to this therapeutic modality is a major clinical problem. Here we show that miR-139-5p is a potent modulator of radiotherapy response in breast cancer via its regulation of genes involved in multiple DNA repair and reactive oxygen species defense pathways. Treatment of breast cancer cells with a miR-139-5p mimic strongly synergized with radiation both *in vitro* and *in vivo*, resulting in significantly increased oxidative stress, accumulation of unrepaired DNA damage, and induction of apoptosis. Several miR-139-5p target genes were also strongly predictive of outcome in radiotherapy-treated patients across multiple independent breast cancer cohorts. These prognostically relevant miR-139-5p target genes were used as companion biomarkers to identify radioresistant breast cancer xenografts highly amenable to sensitization by cotreatment with a miR-139-5p mimetic.

Significance: The microRNA described in this study offers a potentially useful predictive biomarker of radiosensitivity in solid tumors and a generally applicable druggable target for tumor radiosensitization. *Cancer Res; 78(2); 501–15. ©2017 AACR.*

Downloaded from http://aacrjournals.org/cancerres/article-pdf/78/2/501/2772847/501.pdf by guest on 26 August 2022

Introduction

Radiotherapy is an essential component of primary, adjuvant, and palliative treatment for almost all types of solid cancer. In breast cancer, radiotherapy alone is responsible for decreasing the 10-year risk of recurrence by one half and the 15-year risk of breast cancer–related death by one sixth in early-stage patients (1). Although radiotherapy is a local treatment modality, it also has a profound benefit in preventing systemic dissemination (1). Despite this, local control of the disease still fails in 8%–15% of radiotherapy-treated patients. Because breast tumor cells display a striking range of sensitivities to radiation (2), in many cases locoregional recurrence is thought to be due to the presence or evolution of radioresistant tumor cells for which standard fractionated radiotherapy doses are sublethal. Suboptimal treatment also results from the dearth of radiotherapy-predictive biomarkers available for routine clinical use able to indicate optimal radiation dosing (3). Innate or acquired resistance to radiotherapy leading to treatment failure therefore represents an important clinical problem.

Cellular exposure to radiation results in damage to DNA and other cellular structures that triggers a complex cascade of downstream response pathways in both the nucleus and cytoplasm, including the modulation of cell cycle, DNA repair, reactive oxygen species (ROS) defense, cytokine production, and apoptosis. In certain tumor cell subpopulations, these gene networks can be innately biased toward a radioresistant, prosurvival phenotype, for example, via decreased proliferation or accelerated cell-cycle arrest, more efficient or prolonged DNA repair, or dampened apoptotic signaling (4–6). Increasing evidence has shown that miRNAs, as important posttranscriptional regulators of gene expression, have key roles as regulators of many of these processes. miRNAs also play central roles in therapeutic response in cancer (7), and may also represent both an important new class of prognostic and predictive biomarkers (8), as well as viable therapeutic targets (9). Previous studies have identified important roles of specific miRNAs in radiation response in several cancers, including non–small cell lung (10)

[1]Cancer Research Division, The Kinghorn Cancer Centre/Garvan Institute of Medical Research, Sydney, New South Wales, Australia. [2]St Vincent's Clinical School, Faculty of Medicine, University of New South Wales, Sydney, New South Wales, Australia. [3]Department of Anatomical Pathology, South Eastern Area Laboratory Service (SEALS), St George Hospital, Sydney, New South Wales, Australia. [4]Faculty of Medicine, University of New South Wales, Sydney, New South Wales, Australia. [5]Laboratory for the Molecular Biology of Leukemia, Center for Human Genetics, KU Leuven and Center for the Biology of Disease, VIB, Leuven, Belgium. [6]The Chris O'Brien Lifehouse, Sydney, New South Wales, Australia. [7]Department of Tissue Pathology and Diagnostic Oncology, Royal Prince Alfred Hospital, Sydney, New South Wales, Australia. [8]Sydney Medical School, University of Sydney, Sydney, New South Wales, Australia. [9]Growth Factor Group, Cancer Research UK, Molecular Oncology Laboratories, Weatherall Institute of Molecular Medicine, University of Oxford, John Radcliffe Hospital, Headington, Oxford, United Kingdom. [10]St Vincent's Centre for Applied Medical Research, Darlinghurst, New South Wales, Australia.

Note: Supplementary data for this article are available at Cancer Research Online (http://cancerres.aacrjournals.org/).

Corresponding Author: Timothy J. Molloy, St Vincent's Centre for Applied Medical Research, Level 8, 405 Liverpool St, Darlinghurst, New South Wales 2010, Australia. Phone: 292-954-927; Fax: 292-954-928; E-mail: t.molloy@amr.org.au

doi: 10.1158/0008-5472.CAN-16-3105

©2017 American Association for Cancer Research.

and prostate (11). On the basis of this knowledge, we hypothesized that there may be several as yet undiscovered miRNAs with key roles in mediating the clinically important processes of radiotherapy resistance in breast cancer. We therefore aimed to identify such miRNAs, and to determine whether they and/or their targets could represent viable drug targets and biomarkers suitable for future clinical exploitation.

Materials and Methods

Clinical specimens

Primary breast tumor specimens were collected during surgery for breast cancer from patients enrolled in the St. George Breast Boost trial conducted at St. George Hospital (Sydney, New South Wales, Australia). Studies were performed after approval by the institutional review board (human research ethics committee) of St. George Hospital (approval 96/84) and in accordance with the Declaration of Helsinki, and informed written consent was obtained from all subjects where necessary. Formalin-fixed paraffin embedded tumor material from 20 patients was collected, consisting of two groups of 10 patients matched for all clinicopathologic variables and differing only in local relapse status, with a median follow-up time of 9 years (see Supplementary Table S1, for full clinicopathologic characteristics). Radiotherapy consisted of 45 Gy in 25 fractions plus a tumor bed boost of 16 Gy in 8 fractions. miRNA was extracted from tissue samples using the mirVana miRNA Isolation Kit (Ambion) as per the manufacturer's instructions. miRNA quality and quantity was determined by spectrophotometry.

miRNA and mRNA microarray analysis

miRNA and mRNA profiling of primary breast tumor specimens and cell lines was performed using Human (V3) 8 × 15K miRNA microarrays (Agilent), based on Sanger miRbase release 12, and SurePrint G3 Human GE 8 × 60K Microarrays (Agilent), respectively. Labeling and hybridization of microarrays was performed by the Ramaciotti Centre for Genomics (University of New South Wales, Sydney, New South Wales, Australia). Following data extraction and normalization using Agilent microarray scanning software, analyses were performed using BRB-ArrayTools (developed by Dr. Richard Simon and the BRB-ArrayTools Development Team) and in the R statistical computing and graphics environment (http://www.r-project.org). After averaging probes across each array and excluding probes missing in >30% of samples, a significance threshold of 0.001 for univariate testing and a fold-change threshold of 2.0 (miRNA) or 1.5 (mRNA) was used to identify differentially expressed genes. The Gene Expression Omnibus (GEO) accession numbers for miRNA and mRNA expression data are GSE107743 and GSE107800, respectively.

Cell lines and transfections

Cell lines were obtained from ATCC between 2001 and 2012 and cultured according to their recommendations (www.atcc.org). All cell lines were used within approximately 10–50 passages of thawing original stocks, regularly tested for mycoplasma, and authenticated by STR genotyping immediately prior to use. miR-139-5p and negative control miScript mimics and inhibitors (Qiagen) were transfected into cultured cells using the HiPerFect transfection reagent (Qiagen) at a final concentration of 10 nmol/L as per manufacturer's instructions. miScript miRNA Target Protectors (Qiagen), designed to transiently disrupt miR-139-5p binding to each target site, were transfected at a final concentration of 500 nmol/L. mRNA was extracted from cells using the RNEasy Mini Kit (Qiagen) as per manufacturer's instructions. mRNA quality and quantity was determined by spectrophotometry.

Irradiation

Cultured cells and mice were irradiated with the doses specified using the X-RAD 320 X-ray irradiator (Precision X-Ray Inc) at a dose rate of 1 Gy/minute on a rotating pedestal.

Biomarker validation

mRNA/miRNA expression data from publicly available microarray datasets downloaded from the National Center for Biotechnology Information (NCBI) GEO repository and the Molecular Taxonomy of Breast Cancer International Consortium (METABRIC) data portal were used for analysis. Datasets were selected for analysis based on the quality of patient clinicopathologic data available (including treatment information), cohort size, and length of clinical follow up. GEO datasets GSE2034 ("Rotterdam"; $n = 286$; ref. 12), GSE4922 ("Uppsala"; $n = 142$; ref. 13), GSE11121 ("Mainz"; $n = 200$; ref. 14), GSE22220 ("Oxford"; $n = 102$; ref. 15), GSE31863 ("Lund"; $n = 143$; ref. 16), and the METABRIC dataset ($n = 538$; ref. 17) were included in the analysis (Supplementary Tables S2–S4 for patient characteristics). Patients were excluded if they received systemic chemotherapy, did not receive adjuvant radiotherapy, or if treatment was unknown. A minimum *P* value approach was used to select a cut-off point for each biomarker with *P* values corrected for multiple testing (18). Follow-up was capped at 10 years for those datasets with insufficient subsequent survival events for reliable analysis. Data were analyzed and reported according to ReMARK recommendations for studies on tumor markers (19).

Animal studies

All animal experiments were approved by the Institutional Animal Care and Use Committee of the Garvan Institute of Medical Research and the University of New South Wales (Sydney, New South Wales, Australia). To establish breast cancer xenografts, 3×10^6 MCF7 or SKBR3 cells suspended in Matrigel (Corning) were implanted by orthotopic injection into the mammary fat pads of 8- to 12-week-old female Balb/c nude mice. Mice receiving MCF7 xenografts were also supplemented with a subcutaneous slow-release 17β-estradiol pellet (Innovative Research of America). Mimic ± fractionated radiotherapy treatment commenced once a palpable tumor (~150 mm^3) had formed. Delivery efficiency of miRNA mimics via peritumoral subcutaneous injection was first established using Alexa Fluor 488-labeled control mimics. Fluorescence was widespread within the tumor for up to 7 days (the last time point collected), confirming effective delivery via this route of administration. Twenty micrograms of miR-139-5p or negative control miScript mimic (Qiagen) suspended in MaxSuppressor In Vivo RNA-LANCEr II (Bio Scientific) *in vivo* transfection reagent was delivered to animals by pertiumoral subcutaneous injection. Eight hours later, mice were lightly anesthetized before being placed inside a full-body irradiation shield (Braintree Scientific) containing a 10-mm circular hole through which the tumor xenograft was exposed, and treated with 2 Gy radiation. Mice received 4 (MCF7) or 6 (SKBR3) fractionated doses of radiation over 2 or 3 weeks, respectively, with mimics administered prior to the first, third, and fifth (for SKBR3 only) fraction.

Downloaded from http://aacrjournals.org/cancerres/article-pdf/78/2/501/2772847/501.pdf by guest on 26 August 2022

Luciferase assays

The 60bp genomic region containing each predicted miR-139-5p binding site was cloned either downstream (for 3′ UTR binding sites) of the *luc2* luciferase reporter gene in the pmiRGlo Dual Luciferase vector (Promega), or upstream (for 5′ UTR binding sites) of the *RenSP* luciferase reporter gene in the pLightSwitch_5UTR vector (Active Motif). Constructs were cotransfected with either the miR-139-5p or control mimic and luciferase signal quantified by spectrometry using either the Dual-Glo Luciferase Assay System (Promega) or LightSwitch Luciferase Assay System (Active Motif) as appropriate, as per manufacturer's instructions.

cDNA synthesis and quantitative real-time PCR

For miR-139-5p quantification, cDNA was prepared using the miScript II RT Kit (Qiagen) and measured using the TaqMan Small RNA Assay and TaqMan PCR Mastermix (Applied Biosystems) as per the manufacturer's instructions. For mRNA quantification, cDNA was generated from total RNA using the SuperScript VILO cDNA Synthesis Kit (Life Technologies) and measured using the Roche Universal Probe Library and Mastermix on the LightCycler 480 qPCR system (Roche Diagnostics) as per the manufacturer's instructions. qPCR primer sequences and corresponding Universal Probe Library Probe numbers are shown in Supplementary Table S5.

Antibodies

MAT2A, POLQ, TOP2A, RAD54L, XRCC5, γH2AX, Ki-67, cleaved caspase-3, GAPDH, and β-actin antibodies were purchased from Sigma-Aldrich. TOP1 antibody was purchased from Invitrogen Life Technologies.

Functional assays

CellTiter 96 Aqueous One Solution Cell Proliferation Assay (MTS) Assay (Promega), DNA Damage AP Sites Colorimetric Assay Kit (Abcam), glutathione (GSH)/GSSG-Glo Assay (Promega), CellROX Green oxidative stress detection reagent (Thermo Fisher Scientific), Apo-ONE Homogeneous Caspase-3/7 Assay (Promega), and ApoTox-Glo Triplex Apoptosis Assay (Promega) were performed as per manufacturer's instructions.

Statistical analysis

Statistical analyses were performed using Prism 9 (GraphPad) and PASW Statistics 18 (SPSS). All results were confirmed in at least three independent experiments. Quantitative data are presented as mean ± SD unless otherwise denoted. Student *t* tests were used for the comparison of means of quantitative data between groups. Two-way ANOVA was used to compare dose–response curves. Univariate and multivariate Cox regression analyses and Kaplan–Meier plots were used for survival analyses in which endpoints were isolated local recurrence, distant relapse–free survival, recurrence-free survival, overall survival, and disease-specific survival as defined by the STEEP criteria (20). *P* values <0.05 were considered statistically significant and all tests were two-sided.

Results

Multiple miRNAs are associated with local relapse in patients with radiotherapy-treated breast cancer

Primary tumor specimens from early-stage breast cancer patients previously enrolled into a randomized radiotherapy clinical trial (21) were selected for miRNA microarray profiling. Patients treated with breast conserving surgery (BCS) + radiotherapy but no chemotherapy were equally divided into two groups matched for all clinicopathologic variables (Supplementary Table S1) barring local relapse status (median follow up time 9 years). Microarray profiling was used to identify miRNAs associated with local relapse following radiotherapy with the aim of also enriching for miRNAs associated with radiotherapy resistance or sensitivity. Eleven miRNAs were significantly differentially expressed between the two groups (at <0.001 level by univariate test and FDR <5%; Fig. 1A). StarBase (22) was used to predict putative target genes for each. miR-139-5p, overexpressed 3.8-fold in the tumors of nonrelapsed patients, was chosen for further study as it was predicted to target the largest number of genes that have potentially important roles in radiation response, including those associated with DNA repair and maintenance (TOP1, TOP2A, XRCC5, RAD54L, RAD54L2, POLQ, UBE2N, CDT1, SEPT6), cell-cycle control and proliferation (FOS, ZEB2, LAPTM4B), ROS defense (MAT2A), and apoptosis (TP53INP1). miR-139-5p expression was also significantly elevated in the tumors of radiotherapy-treated patients from two additional independent cohorts consisting of 538 and 207 breast cancer patients (15, 17) who had excellent outcome (no relapse or death; Fig. 1B and C; $P < 0.05$; mean follow-up time 8.2 and 7.8 years, respectively). Together these data support a role for miR-139-5p in the tumor response to radiotherapy.

miR-139-5p regulates radiation sensitivity in breast cancer cells

We next sought to determine whether exogenous miR-139-5p could increase radiation sensitivity *in vitro*. MCF7 breast cancer cells were selected as the initial *in vitro* model as they share the same intrinsic subtype as the patients profiled (Luminal A) and have a very well-characterized DNA damage response (DDR) and DDR-related gene mutation status. Cells transfected with a miR-139-5p mimic (which increased intracellular levels by several hundred-fold) and exposed to a 0 to 12Gy radiation demonstrated significantly decreased survival compared to negative control mimic-transfected control cells, corresponding to a mean increase in sensitivity of 52% by MTS assay (day 4; Fig. 1D; $P < 0.01$). Cell death often occurs over an extended period following a single radiation exposure. Clonogenic assays demonstrated that miR-139-5p's inhibitory effects were present for an extended period, with transfected cells forming up to 80% fewer colonies 14-days posttreatment compared to controls (Fig. 1E; $P < 0.001$). miR-139-5p mimic transfection also sensitized MCF7 cells to a fractionated radiation dose (four 2-Gy doses over 8 days), which more closely reflects dosing in the clinic (Supplementary Fig. S1A and S1B). Strong sensitization effects were not only specific to radiation-induced damage—miR-139-5p also significantly sensitized cells to a range of DNA-damaging chemotherapeutics (cisplatin, mitomycin C, doxorubicin, and particularly the PARP inhibitor rucaparib; Fig. 1F–I). In addition, endogenous miR-139-5p levels were also inversely correlated to sensitivity to these and 11 other DNA-damaging compounds (Supplementary Table S6). These findings potentially broaden the clinical relevance of miR-139-5p and suggest it may also have a role in the response to several other important DNA-damaging agents currently in use for the treatment of a wide range of cancers.

Although exogenous miR-139-5p had clear radiosensitization effects, importantly at physiologic levels miR-139-5p was also

Downloaded from http://aacrjournals.org/cancerres/article-pdf/78/2/501/2772847/501.pdf by guest on 26 August 2022

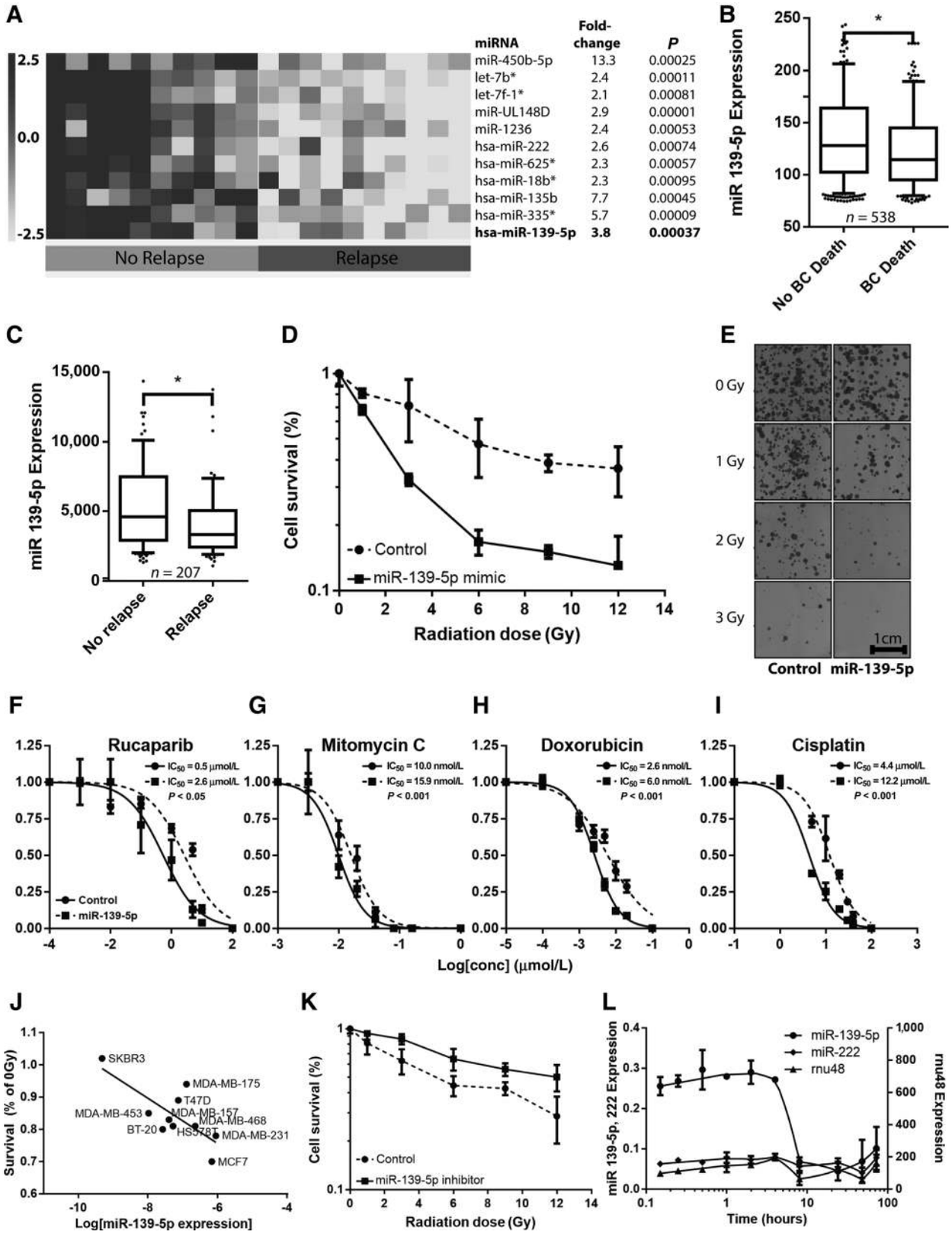

Downloaded from http://aacrjournals.org/cancerres/article-pdf/78/2/501/2772847/501.pdf by guest on 26 August 2022

significantly negatively correlated with radiation resistance, as measured across 10 breast cancer cell lines ($r^2 = 0.55$ Fig. 1J; $P = 0.0138$). In addition, inhibiting basal miR-139-5p expression in MCF7 cells by transfection with a miR-139-5p inhibitor conferred significant resistance to radiation compared with controls (Fig. 1K; $P < 0.05$). Quantitation of endogenous miR-139-5p demonstrated that its expression itself was also radiation-responsive—basal miR-139-5p expression was rapidly downregulated following irradiation, with a 75% decrease 4 to 8 hours after a single 3-Gy dose (Fig. 1L). This compares to miR-222, which was also differentially expressed in the initial patient cohort (Fig. 1A), and a third miRNA, rnu48, neither of which showed significant time-dependent changes in gene expression.

miR-139-5p directly targets critical DNA repair and ROS defense genes

miRNAs exert their effects through posttranscriptional silencing, most often by binding to untranslated regions (UTR) of target mRNAs by complimentary base pairing (23). To identify the gene targets of miR-139-5p that may be responsible for its radiosensitization effects, we used an integrative genome-wide bioinformatics approach (Fig. 2A). First, putative miR-139-5p targets were identified from three sources: CLIP-Seq experimentally supported miRNA-mRNA target prediction datasets generated by starBase v2.0 (22), enriched targets identified from miR-139-5p pulldown experiments (24) and target prediction by the RNA22 algorithm (25). Second, this combined putative target list was filtered by siRNA screen data derived from three independent studies that identified genes whose loss of function was associated with radiation sensitivity (26–28). Third, these data were compared with significantly downregulated genes identified by microarray gene expression profiling of miR-139-5p mimic-transfected MCF7 cells (Fig. 2A). In this manner, 13 genes were identified that were predicted targets of miR-139-5p, downregulated following miR-139-5p mimic transfection, and when downregulated, triggered sensitivity to ionizing radiation. The predicted binding site of 11 of the 13 putative targets was in the 3′ and/or 5′ UTR region of each gene, whereas 2 were present in the coding domain sequence (CDS). Luciferase reporter constructs confirmed miR-139-5p binding to 4 of the 11 genes containing UTR binding sites: MAT2A, POLQ, TOP1, and TOP2A (Fig. 2B). The expression of these 4 genes was also downregulated at both the mRNA and protein level in response to miR-139-5p mimic transfection (Fig. 2C–E). In addition, two further genes with putative binding sites in their CDS regions, XRCC5 and RAD54L, were also significantly downregulated at the mRNA (RAD54L) and protein (RAD54L and XRCC5) level. The cotransfection of miRNA target protectors, designed to transiently disrupt miR-139-5p binding to each target site, efficiently reversed the repression of gene expression, further confirming binding at the sites predicted (Fig. 2C). Comparative genomics of predicted miR-139-5p binding sites demonstrated the strong evolutionary conservation of all six binding sites across 15 eutherian mammals (Supplementary Fig. S2A), consistent with these short regulatory sequences having functional significance across diverse species. Finally, paired mRNA/miRNA profiling of 207 primary breast cancer tumors (GEO dataset GSE22220; ref. 15) demonstrated that the endogenous expression of all genes barring XRCC5 showed a negative linear correlation to basal miR-139-5p expression, which was particularly strong for POLQ, TOP2A, and RAD54L (Fig. 2F–H; Supplementary Fig. S2B–D). This provides evidence that miR-139-5p plays an important role in the regulation of these genes at physiologic levels in breast tumors and not only when artificially overexpressed. Together, these data demonstrate that miR-139-5p directly regulates critical DNA maintenance and repair genes POLQ, TOP1, TOP2A, RAD54L, and XRCC5, and ROS defense-related gene MAT2A.

miR-139-5p overexpression inhibits DNA repair and oxygen-free radical scavenging, leading to apoptosis in irradiated breast cancer cells

Microarray gene expression profiling of mimic-transfected MCF7 cells was undertaken to identify potential signaling pathways responsible for miR-139-5p–mediated radiosensitization. In accordance with the nature of the targets identified, Ingenuity Pathway Analysis (IPA; Qiagen) identified "DNA Recombination, Replication, and Repair and Cancer" among the top three differentially expressed networks, with 19 of the 25 (76%) differentially expressed genes assigned to the network being significantly downregulated (Fig. 3A). Central signaling nodes in this network were key stress response genes PRKAA1/2 (AMPK1/2), and TP53, which together closely link DNA repair-related (POLQ, TOP1, TOP2A, RAD54L, and XRCC5) and ROS defense-related (MAT2A) miR-139-5p target genes in a single gene network. To determine whether these findings had functional significance, we next quantified the DNA repair ability of mimic-transfected following irradiation. Phosphorylated histone protein γH2AX (phospho-H2AX) rapidly (<1 minute) binds to DNA double-stranded breaks (DSB), forming a scaffold for the assembly of DDR proteins, and is a marker of unrepaired radiation-induced DNA damage (29). Consistent with strongly inhibited DNA repair, phospho-H2AX levels

Downloaded from http://aacrjournals.org/cancerres/article-pdf/78/2/501/2772847/501.pdf by guest on 26 August 2022

Figure 1.

High miR-139-5p expression is associated with improved breast cancer patient outcome following radiotherapy, and overexpression of miR-139-5p sensitizes MCF7 cells to radiation. **A,** miRNA genes associated with local relapse in the primary tumors of radiotherapy-treated breast cancer patients and their mean fold-change in no relapse vs. relapse samples. **B-C,** miR-139-5p was significantly upregulated in breast cancer patients who did not experience relapse or death (respectively) following radiotherapy in two independent cohorts ($n = 538$ and 207). **D** and **E,** Exogenous miR-139-5p expression significantly sensitizes MCF7 breast cancer cells to radiation *in vitro*, as measured by MTS (**D**; $P = 0.004$ by ANOVA) and clonogenic assays (**E**; $P < 0.001$). **F–I,** IC_{50} curves for four genotoxic chemotherapy agents. miR-139-5p mimic transfection not only sensitizes tumor cells to radiation, but also DNA damaging chemotherapeutic drugs (all $P < 0.05$). **J,** Basal miR-139-5p expression was negatively correlated with resistance to a single 3Gy dose of radiation in 10 breast cancer cell lines, as measured by MTS assay 4 days posttreatment (expression values are $\log_2$; $r^2 = 0.55$, $P = 0.01$). **K,** Inhibition of miR-139-5p in MCF7 cells, which have among the highest levels of endogenous miR-139-5p expression of the breast cancer cell lines analyzed, conferred significant resistance to a dose range of radiation ($P = 0.049$). **L,** Basal miR-139-5p expression in MCF7 cells quickly decreases following irradiation (3Gy dose), in contrast to miRNAs-222 and rnu48, which remain little changed (bars, SD). Significance calculated by ANOVA and Student *t* test as appropriate. *, $P < 0.05$; ***, $P < 0.001$.

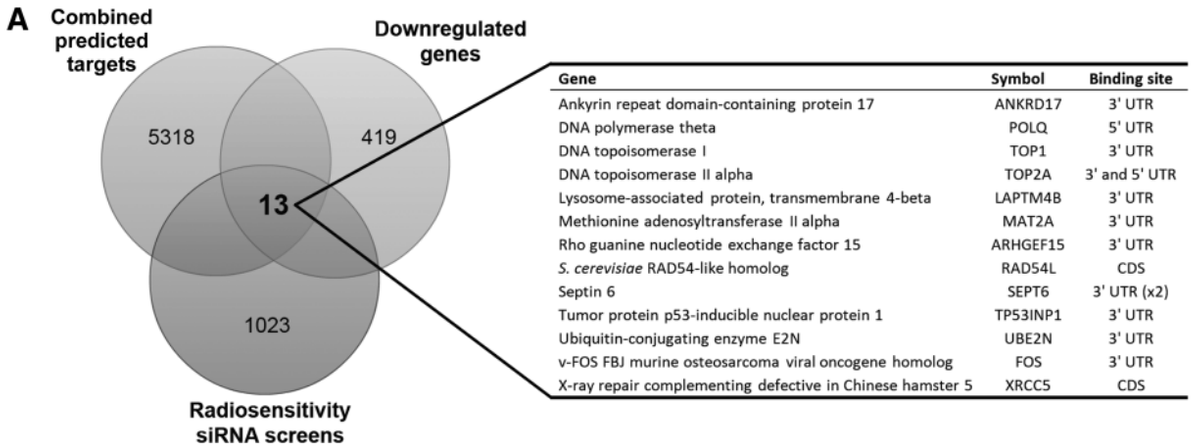

Gene	Symbol	Binding site
Ankyrin repeat domain-containing protein 17	ANKRD17	3' UTR
DNA polymerase theta	POLQ	5' UTR
DNA topoisomerase I	TOP1	3' UTR
DNA topoisomerase II alpha	TOP2A	3' and 5' UTR
Lysosome-associated protein, transmembrane 4-beta	LAPTM4B	3' UTR
Methionine adenosyltransferase II alpha	MAT2A	3' UTR
Rho guanine nucleotide exchange factor 15	ARHGEF15	3' UTR
S. cerevisiae RAD54-like homolog	RAD54L	CDS
Septin 6	SEPT6	3' UTR (x2)
Tumor protein p53-inducible nuclear protein 1	TP53INP1	3' UTR
Ubiquitin-conjugating enzyme E2N	UBE2N	3' UTR
v-FOS FBJ murine osteosarcoma viral oncogene homolog	FOS	3' UTR
X-ray repair complementing defective in Chinese hamster 5	XRCC5	CDS

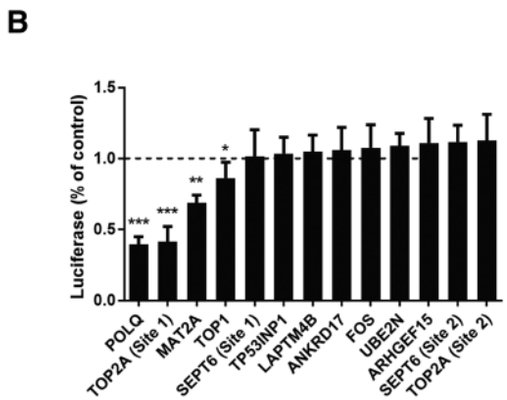

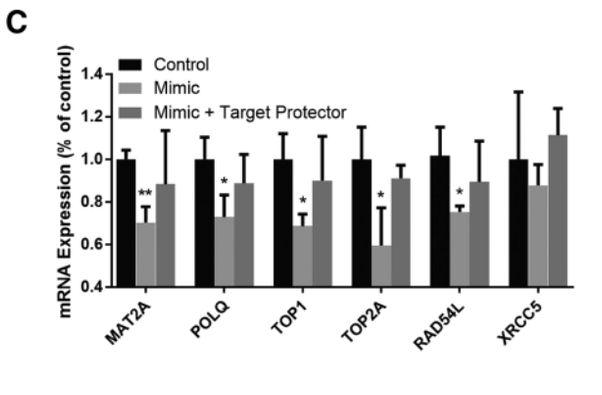

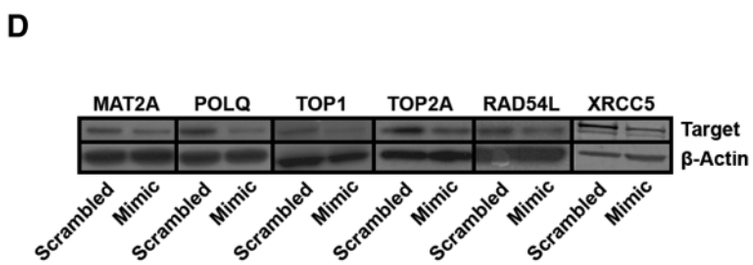

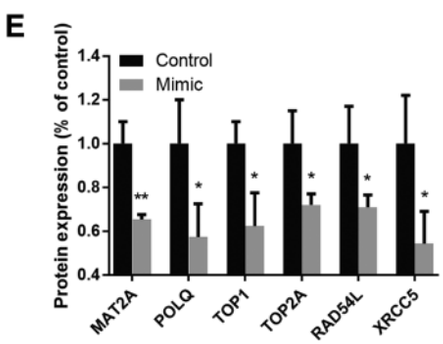

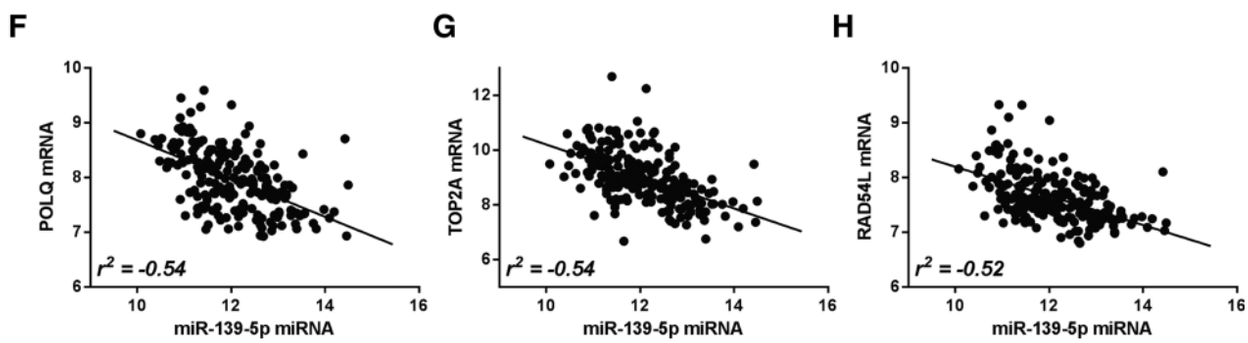

Downloaded from http://aacrjournals.org/cancerres/article-pdf/78/2/501/2772847/501.pdf by guest on 26 August 2022

in miR-139-5p mimic–transfected, irradiated cells increased 3.7-fold compared with control-mimic irradiated cells by 24 hours postirradiation (Fig. 3B; with controls at this time point exhibiting a 1.5-fold increase compared with nonirradiated cells), and remained significantly higher for at least 72 hours (the final time point assayed) as measured by Western blot analysis. Single-cell analyses further revealed a 3-fold increase in nuclear phospho-H2AX foci 24 hours postirradiation (Fig. 3C and D; $P < 0.0001$). Apurinic/apyrimidinic (AP) site formation is a second major indicator of radiation-induced (particularly oxidative) DNA damage, and results in noninstructional lesions that are potentially mutagenic and cytotoxic (30). POLQ and XRCC5 are both required for the efficient removal of AP sites near DSBs (31, 32). Consistent with their repression, an 86% increase in genome-wide AP sites was observed in irradiated mimic-transfected cells versus controls (19.9 vs. 37.1 sites per 10^5 bases; $P < 0.01$; Fig. 3E). To confirm whether miR-139-5p–mediated inhibition of these DNA repair networks would further sensitize DDR-deficient cell lines as expected, and to generalize our findings outside the MCF7 cell line, an additional nine breast cancer lines with varying complements of DDR-related mutations and DNA damage sensitivities (Supplementary Table S6) were also treated with a radiation dose range (0–12 Gy) and a miR-139-5p or control mimic. miR-139-5p overexpression significantly increased radiation sensitivity in all 10 cell lines, ranging from 18% to 64% at 6Gy (all $P < 0.05$; Fig. 3F and G and Supplementary Fig. S3A–S3I). Although there was no clear relationship between induced sensitivity and intrinsic subtype, there was a positive association between induced sensitivity and the number of pathogenic mutations in key DDR genes (which itself was associated with endogenous sensitivity to 15 DNA-damaging agents; Supplementary Table S6): the average sensitivity of cell lines with >1 mutation increased by a mean 42% in response to miR-139-5p overexpression, compared with a mean 24% in those cell lines with $\leq$1 mutation ($P = 0.018$). Overall, transfection with the miR-139-5p mimic was twice as potent in promoting radiation sensitivity compared to accumulating 2 or more DDR mutations. These data are consistent with miR-139-5p's ability to inhibit multiple DDR pathways simultaneously, which compounds with mutations in DDR-related genes to induce radiation sensitivity in these cell lines.

The activity of central DDR signaling node PRKAA is regulated by S-adenosylmethionine (SAM; ref. 33), biosynthesis of which is catalyzed by miR-139-5p target MAT2A. SAM synthesis also contributes to defense against the highly genotoxic ROS generated by ionizing radiation, which is the major catalyst of both DSBs and AP sites (34). miR-139-5p mimic transfection significantly sensitized cells to the ROS generator menadione [IC_{50} values of 3.3 and 5.9 μmol/L for control and mimic-transfected cells, respectively ($P < 0.001$); Supplementary Fig. S3J]. In addition, significantly increased oxidation of the CellROX Green fluorogenic oxidation probe was observed in mimic-transfected irradiated cells compared with controls (Fig. 3H and I), as was well a significant increase in the intracellular level of the oxidized form of major antioxidant glutathione (GSSG; Fig. 3J), both suggesting that cells were experiencing markedly increased oxidative stress.

Finally, the increased oxidative stress and accumulation of unrepaired DNA damage preceded the strong activation of apoptosis effector proteins caspases 3/7, particularly at higher radiation doses (with a 3.2-fold higher caspase-3/7 activation compared with controls at 15Gy; Fig. 3K), which coincided with the observed increased cytotoxicity in miR-139-5p mimic-transfected and irradiated cells (Fig. 1D and E). Together, these data indicate that miR-139-5p targets key members of multiple signaling pathways associated with the response to ionizing radiation damage. This results in significantly inhibited DNA repair, free radical scavenging, and the promotion of apoptotic cell death, consistent with its novel role as a radiotherapy sensitizer.

miR-139-5p and its targets are strong predictive biomarkers for radiotherapy

Because miR-139-5p and several of its validated targets were confirmed to be important mediators of radiation sensitivity *in vitro*, we next hypothesized that these genes may also make effective clinical biomarkers to predict patient outcome following radiotherapy. To determine this, tumor expression of miR-139-5p and each of its targets was correlated to clinical outcome in 1,268 stage I–III breast cancer patients who were treated with surgery + adjuvant radiotherapy (no chemotherapy), derived from five independent, retrospective microarray gene expression datasets with long-term clinical follow-up ["Rotterdam"; $n = 286$; ref. 12), "Uppsala" ($n = 142$; refs. 13, 35), "Mainz" ($n = 200$; ref. 14) for mRNA, and "Oxford" ($n = 102$; ref. 15), and "METABRIC" ($n = 538$; ref. 17) for miRNA; Supplementary Tables S2–S4, for patient characteristics). The expression of miR-139-5p and three of its targets, POLQ, TOP2A, and RAD54L, proved to be strongly correlated to disease-free survival (DFS), distant metastasis-free survival (DMFS), and breast cancer–specific survival (BCSS) across multiple independent datasets [Fig. 4A–D; miR-139-5p HR 0.3–0.5, $P < 0.05$; RAD54L, TOP2A, and POLQ HRs 2.2–3.4, 2.8-5.2, and 2.6-4.2, respectively; all $P < 0.05$ (excluding RAD54L

Downloaded from http://aacrjournals.org/cancerres/article-pdf/78/2/501/2772847/501.pdf by guest on 26 August 2022

Figure 2.

miR-139-5p directly targets critical DNA repair and ROS defense genes. **A,** Putative miR-139-5p target genes relevant to radiotherapy response were identified by taking the overlap between bioinformatically predicted or experimentally validated targets, genes that triggered radiation sensitivity in three siRNA screens, and genes that were identified by microarray gene expression profiling as being downregulated at least 1.5-fold in response to miR-139-5p mimic transfection. Thirteen putative targets were identified that passed all three filters. **B,** Luciferase signal was quantified in MCF7 cells cotransfected with a luciferase expression construct containing the predicted miR-139-5p binding site from each putative target gene and the miR-139-5p mimic. Values represent the change in luciferase signal detected compared with controls. **C** and **D,** Five of the six putative targets were significantly downregulated at the mRNA level in response to miR-139-5p mimic transfection (compared with cells transfected with a negative control mimic; measured by qPCR; **C**), and all six putative targets were significantly downregulated at the protein level (measured by Western blotting; **D** and **E**). Cotransfection with target protectors, which specifically bind to and block each putative miR-139-5p binding site, reversed the effects on mRNA repression and resulted in expression not significantly different from controls (**C**; $n = 4$–6). **F–H,** Paired mRNA/miRNA gene expression profiling data of the primary tumors of 207 breast cancer patients (15) demonstrated that the endogenous expression of POLQ (**F**), TOP2A (**G**), and RAD54L (**H**) showed a strong negative linear correlation to basal miR-139-5p expression. Bars, SD. Significance calculated with Student *t* test. *, $P < 0.05$; **, $P < 0.01$; ***, $P < 0.001$.

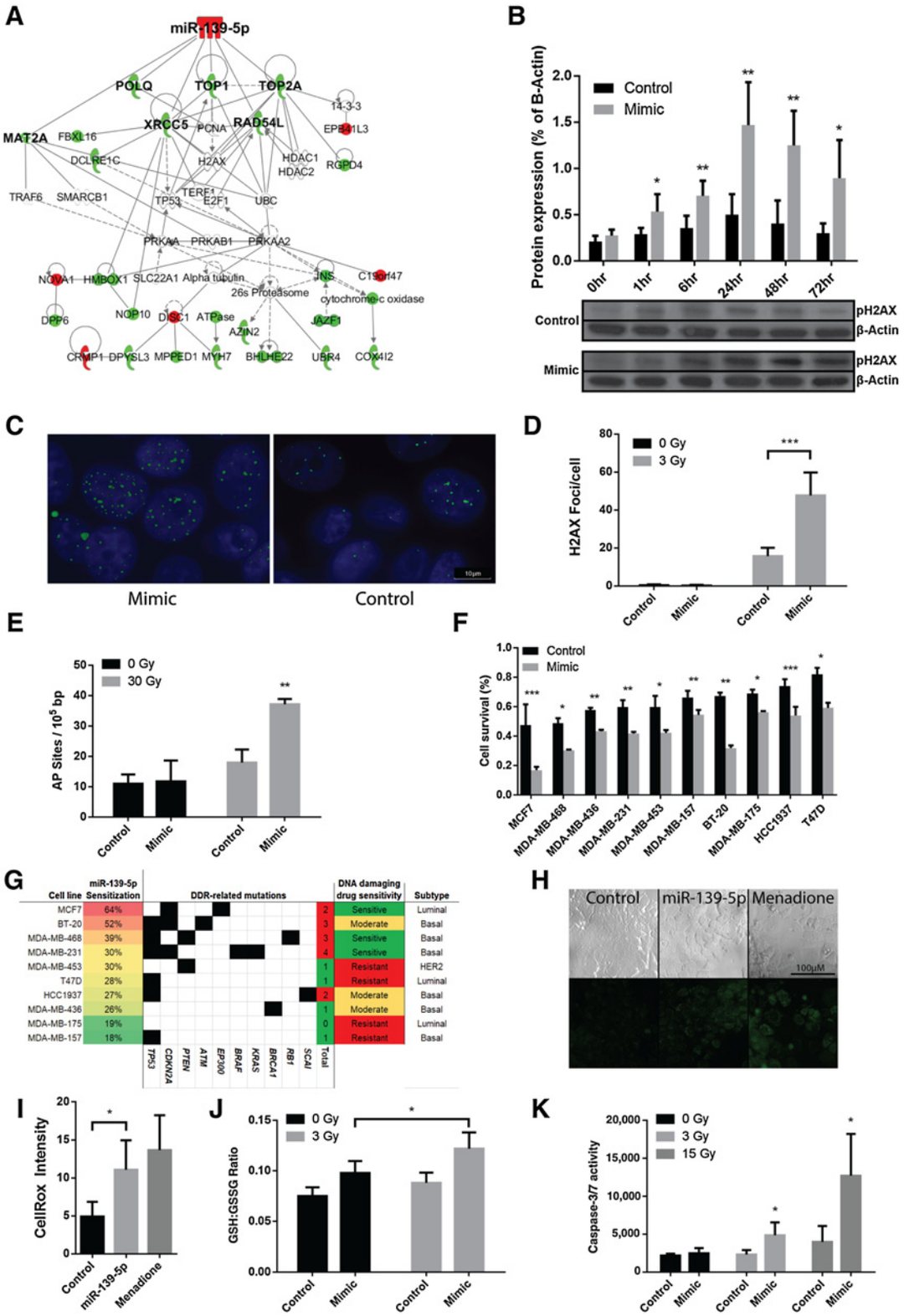

Downloaded from http://aacrjournals.org/cancerres/article-pdf/78/2/501/2772847/501.pdf by guest on 26 August 2022

for DFS in the Uppsala cohort)]. Furthermore, multivariate Cox regression analyses demonstrated that all four genes provided prognostic information independent of all standard clinicopathologic variables tested, including lymph node involvement, tumor size, histologic grade, hormone receptor expression, and age (where data was available) across all cohorts and survival types (excluding RAD54L for DFS in the Uppsala cohort; Table 1).

To distinguish whether these genes were true radiotherapy-predictive rather than simply prognostic biomarkers, a sixth independent cohort ("Lund"; $n = 143$; ref. 16) derived from patients enrolled in a randomized radiotherapy clinical trial and a population-based cohort study with a nested case–control study was analyzed. This cohort consisted of two patient subgroups matched for all clinicopathologic variables (age, tumor size, lymph node involvement, histological grade, ER status, and PR status), one of which received BCS + postoperative radiotherapy and the other treated with BCS alone. TOP2A, POLQ, and particularly RAD54L were all significantly prognostic specifically in radiotherapy-treated [RAD54L and TOP2A for relapse-free survival (RFS), DMFS, and OS, and POLQ for RFS; all $P < 0.05$] but not nonradiotherapy-treated patients, consistent with these genes being true radiotherapy-predictive biomarkers (Fig. 4C and D).

miR-139-5p is a highly effective radiotherapy sensitizer for breast cancer *in vivo*, whereas its targets are companion biomarkers

We next wished to determine whether the miR-139-5p mimic would make an effective radiotherapy sensitizer *in vivo*. MCF7 orthotopic xenografts in BALB/c nude mice were therefore treated with fractionated radiotherapy ± either a miR-139-5p or control mimic (Fig. 5A). As expected, radiotherapy alone was effective in reducing tumor size compared to non-radiotherapy–treated controls (either with or without miR-139-5p mimic), which were all euthanized by day 37 posttreatment due to high tumor burden (>600 mm^3; vs. mean 34 mm^3 for radiotherapy-only treated tumors at this time point; $P < 0.001$; Fig. 5B). After a strong initial response however, radiotherapy-only–treated tumors quickly relapsed, with all tumors reaching >600 mm^3 by day 141. Consistent with our *in vitro* findings, combining fractionated radiotherapy with the miR-139-5p mimic was highly effective, completely eliminating detectable tumors in all mice within 88 days, with animals remaining tumor-free until the final follow up point at Day 250 (Fig. 5C). In agreement with other studies (36), mimic administration appeared to have minimal toxicity, with an additional cohort of mice ($n = 8$) treated with the mimic only (no radiotherapy) displaying no differences in weight, blood cell counts, gross kidney and liver histology, or behavior compared to saline-treated animals 7 days posttreatment (data not shown).

The use of miRNA mimics or inhibitors as therapeutics raises the intriguing possibility that their targets may be used as companion biomarkers, which could indicate their application. Prognostic miR-139-5p targets TOP2A, POLQ, and RAD54L were therefore quantified by qPCR in a panel of 10 breast cancer cell lines to identify those with high expression (and therefore predicted to be radioresistant) versus those with low expression (and therefore predicted to be radiosensitive; Fig. 5D). When summed ranks were compared to endogenous radioresistance, a moderate positive correlation was observed (Fig. 5E). This approach identified the SKBR3 cell line, which expresses high levels of TOP2A, POLQ, and RAD54L (and low levels of miR-139-5p; Fig. 1D), as an optimal candidate for mimic treatment (Fig. 5A). Confirming the *in vitro* findings, SKBR3 xenografts were highly radioresistant, with all radiotherapy-only treated tumors reaching ethical endpoint by day 54, just 25 days after tumors that received no radiotherapy (vs. day 141 for radiotherapy-treated MCF7 xenografts, $P < 0.001$; Fig. 5F). miR-139-5p mimic administration again proved to be highly effective even in these strongly radioresistant tumors, with all treated tumors becoming undetectable by day 205 and all mice surviving to the final follow up point at day 250 (Fig. 5G).

Confirming the *in vitro* findings, radiotherapy + miR-139-5p mimic-treated tumors had significantly decreased Ki-67-positive cells, and significantly increased phospho-H2AX- and caspase-3-positive cells compared with control mimic-treated tumors, consistent with strongly inhibited DNA repair, leading to inhibited proliferation and activated apoptosis (Fig. 5H–J and Supplementary Fig. S4A–C). Importantly, phospho-H2AX immunostaining was confined to the tumor field that received the radiation; the kidneys and liver, nontarget organs that were not within the radiation field, but which accumulated miRNA mimic, did not have detectable phospho-H2AX expression (Supplementary Fig. S4D and S4E). This indicates that the mimic strongly synergized with radiation, and suggests that systemic administration of miR-139-5p can result in genotoxicity that is highly-targeted to the tumor cells within the radiation field with minimal effects on non-target tissues. Collectively, these data provide evidence

Figure 3.

miR-139-5p overexpression inhibits DNA repair and ROS defense following irradiation. **A,** IPA was performed on microarray gene expression profiling data from miR-139-5p mimic-transfected (vs. control mimic-transfected) MCF7 cells. The "DNA Recombination, Replication, and Repair and Cancer" network (shown) was among the top three most differentially expressed (green, downregulated; red, upregulated; bold, miR-139-5p targets). **B,** A significant increase in DNA damage marker phospho-H2AX was observed following mimic transfection + 3Gy irradiation compared with controls (Western blot analysis). **C** and **D,** Similarly, visualization of single cells by immunofluorescence revealed a mean three-fold increase in phospho-H2AX foci in miR-139-5p mimic-transfected irradiated cells compared with control transfected irradiated cells (representative image shown 24 hours post-irradiation). **E,** miR-139-5p mimic transfection and irradiation also resulted in significantly increased numbers of AP sites 1-hour post-irradiation. **F** and **G,** Ten breast cancer cell lines were transfected with either a miR-139-5p or control mimic, and exposed to 0 to 12Gy radiation ($n = 3$ biological replicates). miR-139-5p mimic transfection significantly increased sensitivity in all cell lines (all $P < 0.05$ by ANOVA). Sensitization was particularly effective in those cell lines with >1 mutation in key DDR genes (which itself was associated with DNA damage sensitivity as determined by relative response to 15 DNA damaging drugs; Supplementary Table S6). **H** and **I,** Consistent with a downregulation of MAT2A, which catalyses the synthesis of SAM, the CellROX Green flurogenic probe, which exhibits photostable green fluorescence upon oxidation by ROS, was strongly activated in miR-139-5p mimic-transfected versus scrambled control-transfected cells. Positive controls (cells treated with 20 μmol/L menadione, a phosphatase inhibitor and potent free radical producing agent) are also shown as a comparator (green fluorescent intensity quantified in arbitrary units). **J,** Similarly, mimic-transfected and irradiated MCF7 cells displayed a significant increase in oxidative stress as measured by intracellular reduced GSH levels (values shown are relative to total glutathione). **K,** Unrepaired DNA damage in miR-139-5p transfected and irradiated cells preceded a significant increase in caspase-3/7 activation 3 days post-irradiation, compared with controls (data in arbitrary fluorescent units). Bars, SD. Significance calculated with Student *t* test (*, $P < 0.05$; **, $P < 0.01$; ***, $P < 0.001$).

Downloaded from http://aacrjournals.org/cancerres/article-pdf/78/2/501/2772847/501.pdf by guest on 26 August 2022

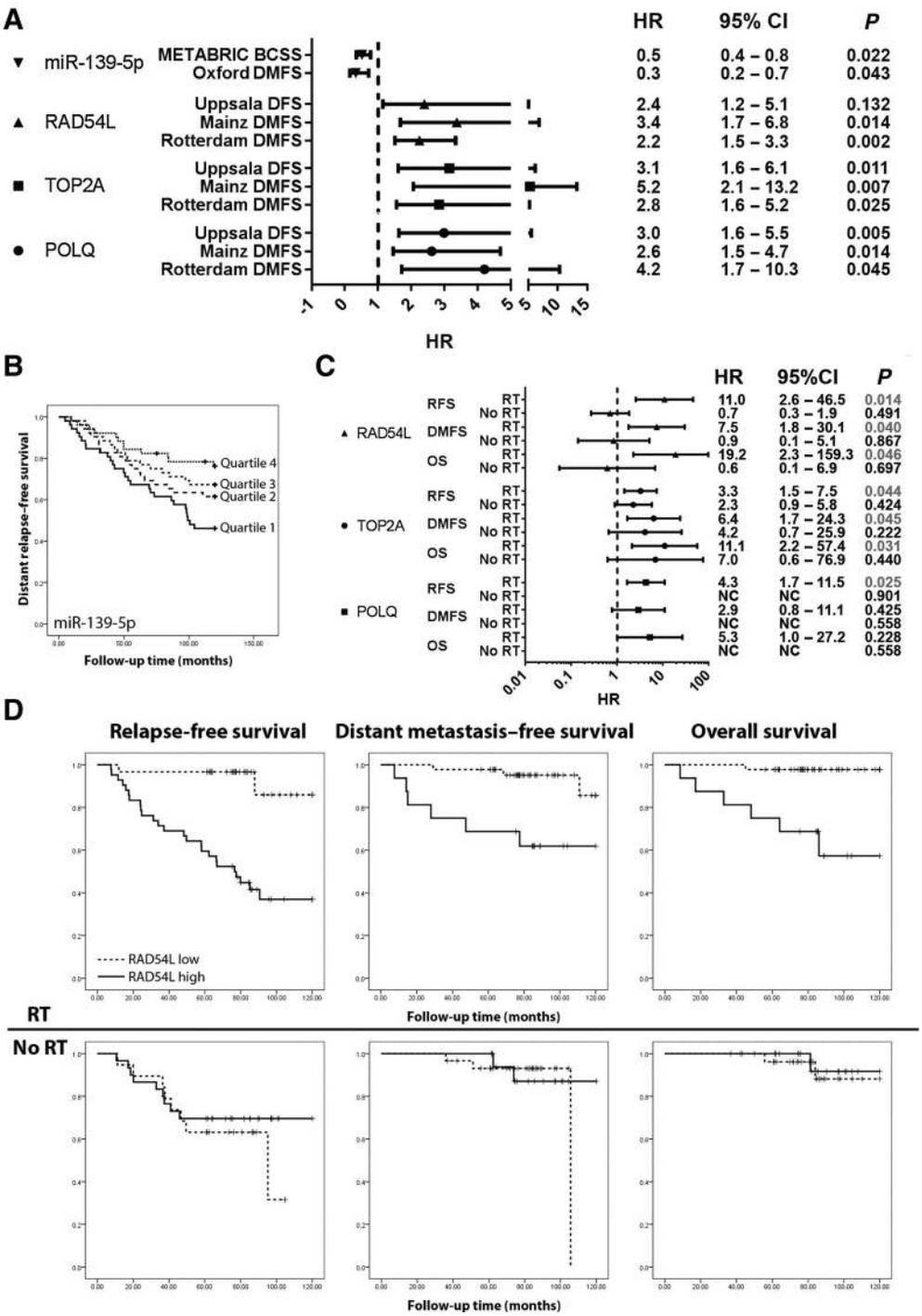

Figure 4.

miR-139-5p and its targets are strong predictive biomarkers for radiotherapy response in breast cancer. **A,** Five independent clinical cohorts ("METABRIC," "Oxford," "Uppsala," "Mainz," and "Rotterdam") totaling 1,268 patients were analyzed, and biomarker expression correlated to outcome. High miR-139-5p expression and low POLQ, TOP2A, and RAD54L expression was consistently and significantly associated with improved survival specifically in patients treated with radiotherapy (no chemotherapy). **B,** Kaplan–Meier plot of miR-139-5p expression (divided into quartiles) versus DMFS from the Oxford cohort. **C,** Gene expression was analyzed from a sixth independent patient cohort ("Lund"; $n = 143$) of matched patients treated with BCS with or without adjuvant radiotherapy (P values > 0.05 are shown in gray). RAD54L and TOP2A for RFS, DMFS, and OS, and POLQ for RFS were significantly prognostic only in radiotherapy-treated patients and not in matched nonradiotherapy–treated patients, consistent with their being true predictive biomarkers for radiotherapy. **D,** Kaplan–Meier plots of RFS, DMFS, and OS in radiotherapy- and nonradiotherapy–treated patients from the Lund cohort for RAD54L, which was a particularly strong and specific radiotherapy-predictive biomarker. NC, not calculable (insufficient survival events).

Downloaded from http://aacrjournals.org/cancerres/article-pdf/78/2/501/2772847/501.pdf by guest on 26 August 2022

Table 1. Multivariate Cox regression demonstrated that miR-139-5p, POLQ, TOP2A, and RAD54L provided significant prognostic information independent of all other clinical variables (for which data was available)

Biomarker	Cohort	Survival type	Clinical variable	HR (95% CI)	*P*
miR-139-5p	METABRIC ($n = 538$)	BCSS	miR-139-5p (high vs low)	0.6 (0.4–1.0)	**0.043**
			Node status (pos vs. neg)	2.3 (1.5–3.6)	0
			Tumor size (>20 mm)	1.6 (1.1–2.5)	**0.029**
			Grade (3 vs. 1/2)	1.3 (0.9–1.9)	0.234
			ER status (pos vs. neg)	0.8 (0.4–1.6)	0.588
			PR status (pos vs. neg)	1.6 (1.0–2.4)	**0.039**
			HER2 status (pos vs. neg)	0.4 (0.3–0.7)	**0.002**
			Age (<55)	1 (0.6–1.5)	0.84
	Oxford ($n = 207$)	DMFS	miR-139-5p (high vs. low)	0.4 (0.2–1.0)	**0.043**
			Node status (pos vs. neg)	2.2 (1.4–3.6)	**0.001**
			Tumor size (>20 mm)	1.7 (1.0–2.8)	0.059
			Grade (3 vs. 1/2)	1.2 (0.7–2.0)	0.422
			ER status (pos vs. neg)	0.6 (0.4–1.0)	0.075
			Age (<55)	1 (1.0–1.1)	**0.001**
POLQ	Uppsala ($n = 142$)	DFS	POLQ (high vs. low)	2.3 (1.1–4.5)	**0.022**
			Node status (pos vs. neg)	1.9 (0.4–9.7)	0.448
			Tumor size (>20 mm)	1.8 (0.9–3.4)	0.072
			Grade (3 vs. 1/2)	2.3 (1.0–5.5)	0.053
			ER status (pos vs. neg)	0.9 (0.4–2.2)	0.891
			Age (<55)	1.1 (0.5–2.1)	0.888
	Mainz ($n = 200$)	DMFS	POLQ (high vs. low)	2.5 (1.3–4.7)	**0.044**
			Tumor size (>20 mm)	0.8 (0.4–1.5)	0.49
			Grade (3 vs. 1/2)	1.9 (1.0–3.6)	0.064
	Rotterdam ($n = 286$)	RFS	POLQ (high vs. low)	4.3 (1.7–10.5)	**0.045**
			ER status (pos vs. neg)	1.1 (0.7–1.7)	0.656
TOP2A	Uppsala	DFS	TOP2A (high vs. low)	2.3 (1.1–4.7)	**0.024**
			Node status (pos vs. neg)	2.4 (0.5–12.1)	0.279
			Tumor size (>20 mm)	1.7 (0.9–3.2)	0.11
			Grade (3 vs. 1/2)	2.6 (1.2–6.1)	**0.022**
			ER status (pos vs. neg)	1 (0.4–2.5)	0.936
			Age (<55)	1.1 (0.5–2.2)	0.864
	Mainz	DMFS	TOP2A (high vs. low)	2.5 (1.3–4.7)	**0.044**
			Tumor size (>20 mm)	0.8 (0.4–1.5)	0.49
			Grade (3 vs. 1/2)	1.9 (1.0–3.6)	0.064
	Rotterdam	RFS	TOP2A (high vs. low)	2.9 (1.6–5.2)	**0.025**
			ER status (pos vs. neg)	1.1 (0.7–1.7)	0.659
RAD54L	Uppsala	DFS	RAD54L (high vs. low)	1.9 (0.7–5.1)	0.202
			Node status (pos vs. neg)	2.9 (0.6–14.5)	0.205
			Tumor size (>20 mm)	1.7 (0.9–3.2)	0.105
			Grade (3 vs. 1/2)	3.9 (1.8–8.7)	**0.001**
			ER status (pos vs. neg)	1.4 (0.5–4.0)	0.536
			Age (<55)	1.3 (0.6–2.6)	0.548
	Mainz	DMFS	RAD54L (high vs. low)	3.1 (1.5–6.4)	**0.021**
			Tumor size (>20 mm)	1 (0.5–1.7)	0.876
			Grade (3 vs. 1/2)	1.8 (1.0–3.6)	0.068
	Rotterdam	RFS	RAD54L (high vs. low)	2.3 (1.6–3.5)	**0.002**
			ER status (pos vs. neg)	1.2 (0.8–1.9)	0.337

NOTE: *P* values > 0.05 are shown in bold.

that miR-139-5p and its targets POLQ, TOP2A, and RAD54L could make a novel and valuable drug target and companion biomarker combination for radiotherapy sensitization in tumors recalcitrant to radiotherapy.

Discussion

Radiotherapy is a central pillar of treatment for almost all types of solid tumor, including breast cancer, with almost half of all cancer patients receiving radiotherapy sometime during their disease course (37). Resistance to radiotherapy leading to treatment failure, compounded by the lack of biomarkers to allow tailoring of radiotherapy to individual tumors, is therefore a critical clinical problem (2, 3). We have demonstrated here for the first time that miR-139-5p may be useful for addressing both of these deficiencies. First, its confirmed targets TOP2A, POLQ, and RAD54L were shown to be predictive biomarkers that could identify radioresistant tumors and predict patients that were likely to have poor outcome following radiotherapy. Second, the use of a miR-139-5p mimic could inhibit the expression of these and other key genes, including TOP1, XRCC5, and MAT2A, to impart sensitivity to even highly radioresistant tumors *in vivo*. Furthermore, miR-139-5p was capable of sensitizing tumor cells to several common DNA damaging chemotherapies. Because targeting DNA is a common treatment strategy across most tumor types, and the development of resistance to these therapies is frequently observed, the clinical relevance of the current findings may be broad.

miR-139-5p has been identified as a tumor suppressor in breast (24), colorectal (38), and esophageal squamous cell

Downloaded from http://aacrjournals.org/cancerres/article-pdf/78/2/501/2772847/501.pdf by guest on 26 August 2022

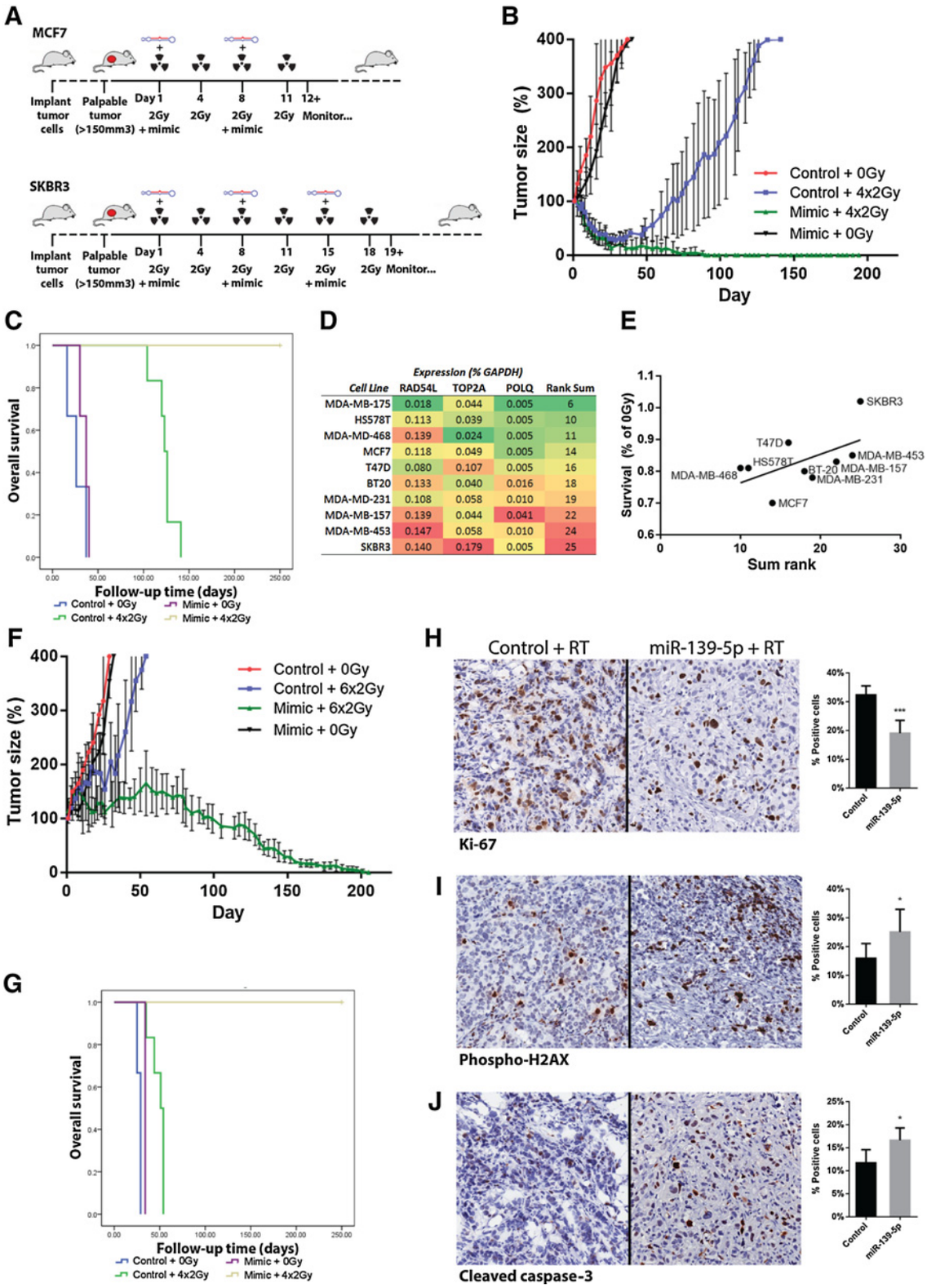

Downloaded from http://aacrjournals.org/cancerres/article-pdf/78/2/501/2772847/501.pdf by guest on 26 August 2022

carcinoma (39), where it has been shown to inhibit migration, invasion, and metastasis. We are the first to report its role in the regulation of key DNA damage response (DDR) genes and as a modulator of radiation resistance. Five of its six confirmed targets have roles in multiple complementary DNA damage response pathways essential for the repair of radiation-induced DNA damage. These pathways include microhomology-mediated end joining [MMEJ; POLQ (40), XRCC5 (41)], base excision repair [BER; POLQ (42)], nonhomologous end-joining [NHEJ; XRCC5 (41)], homologous recombination repair [HR; RAD54L (43)], as well as regulating DNA topology during repair [TOP1 (44), TOP2A (44, 45)]. The sixth target confirmed here, MAT2A, has a role in ROS defense (46).

Although miRNAs often only have moderate effects on the expression of individual target genes, the simultaneous targeting of multiple pathways can result in significant phenotypic changes (47). We have demonstrated that miR-139-5p represses key genes across several redundantly-operable DNA repair pathways, which could explain the significantly higher sensitization to radiotherapy than what might be expected from the mild inhibition of a single gene. For example, Ceccaldi, and colleagues (48) demonstrated that the inhibition of POLQ in ovarian cancer cells resulted in hypersensitivity to DNA damage caused by ionizing radiation and mitomycin C, to which HR-proficient cells responded with a compensatory increase in HR-mediated repair. In HR-deficient tumor cells however, POLQ inhibition resulted instead in strong synthetic lethality. This study further demonstrated that the toxicity induced by POLQ repression in HR-deficient cells was rescued by the co-inhibition of RAD51, suggesting that in the absence of POLQ, RAD51 accumulation is toxic. A second miR-139-5p target, RAD54L, is thought to be involved in mammalian HR-directed DNA repair, chiefly in the removal of RAD51 foci from heteroduplex DNA following strand exchange (43). Simultaneous knockdown of the MMEJ/BER gene POLQ and the HR gene RAD54L by miR-139-5p may therefore act together in causing the accumulation of RAD51 foci and destabilization of the genome. When further combined with inhibited NHEJ activity via XRCC5 repression, multiple DNA damage response pathways that normally show some functional redundancy are suppressed, and thereby synergistically increase sensitivity to radiotherapy-induced DNA damage. This hypothesis is consistent with our finding that miR-139-5p-mediated sensitivity tends to be stronger in those breast cancer cell lines with multiple mutations in DDR genes (Fig. 3f).

The discovery of radiotherapy-specific predictive biomarkers allowing improved individualization of radiation treatment for breast cancer would be of significant value. Standard clinicopathologic variables are suboptimal for accurately predicting which patients will most benefit, resulting in both overtreatment and under treatment of some patients (49). For example, up to 10% of ductal carcinoma *in situ* (DCIS) patients determined to be "low risk" by traditional clinicopathologic variables and therefore not treated with radiation in fact go on to develop either new DCIS or invasive breast cancer (50). These patients would almost certainly benefit from adjuvant radiotherapy. Similarly, of those DCIS patients who are treated with radiotherapy, less than a third would be expected to develop progressive disease in the absence of radiation (51). This overtreatment of good-prognosis patients results in unnecessary toxicity, including a significantly increased chance of developing a new primary tumor in the region (52). Prospective validation of miR-139-5p targets POLQ, TOP2A, and particularly RAD54L, which we are the first to identify as a strong radiotherapy-predictive biomarker for breast cancer, may result in improved selection of patients chosen for radiotherapy in the clinic.

In addition to demonstrating how miRNA targets can be used as both predictive and companion biomarkers, this study has also demonstrated the therapeutic potential of miRNA mimics as therapeutic agents. Although the therapeutic use of nucleic acid-based drugs has been severely hampered by their low stability at physiological pH, short half-lives *in vivo*, and the possibility of off-target effects, this may be less of a stumbling block for miRNA mimics as radiotherapy sensitizers. Transient activity prior to each fractionated radiation dose should be sufficient to "prime" the tumor, making them temporarily susceptible to radiotherapy. Transient activity may also mean decreased toxicity, which is likely already low because the mimic exerts its strongest effects within the highly-targeted field of radiation, and eliminates the risk of long-term unwanted off-target effects. Although the use of miRNA mimics and inhibitors as therapeutic molecules is still in its infancy, there have been a handful of successful nonhuman primate *in vivo* studies and at least one phase I clinical trial that have shown promise, combining efficacy with an acceptable toxicity profile

Downloaded from http://aacrjournals.org/cancerres/article-pdf/78/2/501/2772847/501.pdf by guest on 26 August 2022

Figure 5.

miR-139-5p is a highly effective radiotherapy sensitizer for breast cancer *in vivo*, whereas its targets are companion biomarkers. **A,** *In vivo* treatment schedule. MCF7 or SKBR3 orthotopic xenografts in Balb/c nude mice were treated with a fractionated course of radiation (4 × 2 Gy over 2 weeks for MCF7; 6 × 2 Gy over 3 weeks for SKBR3) targeted to the tumor field ± a miR-139-5p or control mimic, administered 8 hours prior to the first, third (and for SKBR3, fifth) fractions. **B,** Tumor sizes in MCF7 xenograft-bearing Balb/c nude mice treated with a miR-139-5p or control mimic ± fractionated radiotherapy. **C,** Kaplan–Meier survival plot for each MCF7 treatment group. **D,** Expression of miR-139-5p targets and radiotherapy predictive biomarkers POLQ, TOP2A, and RAD54L was measured by qPCR in a panel of 10 breast cancer cell lines. Expression data was ranked and summed to identify cell lines with high expression of biomarkers and therefore predicted to be radioresistant. **E,** Summed ranks correlated to cell line survival 3 days after a single 3 Gy dose of irradiation. Line of best fit is shown calculated with the MDA-MB-175 cell line excluded as an outlier (which showed low biomarker expression but unlike other cell lines was radioresistant). The SKBR3 cell line, which expresses low levels of miR-139-5p and high levels of POLQ, TOP2A, and RAD54L, was highly radioresistant. **F,** Tumor sizes in SKBR3 xenograft-bearing Balb/c nude mice treated with a miR-139-5p or control mimic ± fractionated radiotherapy. **G,** Kaplan–Meier survival plot for each SKBR3 treatment group. **H,** Significantly fewer Ki-67–positive cells were present in the MCF7 xenograft tumors of radiotherapy + miR-139-5p mimic-treated animals compared with radiotherapy + control-treated animals 24 hours after the completion of treatment, indicating inhibited proliferation in these tumors. **I,** Phospho-H2AX expression was significantly higher in radiotherapy + miR-139-5p mimic-treated tumors compared with radiotherapy + control mimic-treated tumors, indicating markedly inhibited DNA repair within these cells. **J,** A significant increase in cleaved caspase-3 was also observed in radiotherapy + miR-139-5p–treated tumors, indicating a strong induction of apoptosis. Bars, SD. Significance calculated with Student *t* test. *, $P < 0.05$; ***, $P < 0.001$.

(9, 53, 54). miR-139-5p may be a good candidate for further investigation as a therapeutic target in similar advanced preclinical studies, not only for breast cancer, but potentially any solid tumor for which DNA damaging agents are a primary treatment modality.

Disclosure of Potential Conflicts of Interest

No potential conflicts of interest were disclosed.

Authors' Contributions

Conception and design: E. Millar, S.A. O'Toole, A.L. Harris, T.J. Molloy
Development of methodology: S. Daly, S.A. O'Toole, G.E. Hollway, T.J. Molloy
Acquisition of data (provided animals, acquired and managed patients, provided facilities, etc.): M. Pajic, D. Froio, S. Daly, E. Millar, P.H. Graham, A. Drury, A. Steinmann, A. Boulghourjian, A. Zaratzian, S. Carroll, S.A. O'Toole, H.E. Gee, T.J. Molloy
Analysis and interpretation of data (e.g., statistical analysis, biostatistics, computational analysis): D. Froio, L. Doculara roio, C.E. de Bock, S.A. O'Toole, A.L. Harris, F.M. Buffa, H.E. Gee, G.E. Hollway, T.J. Molloy
Writing, review, and/or revision of the manuscript: M. Pajic, D. Froio, S.A. O'Toole, A.L. Harris, H.E. Gee, G.E. Hollway, T.J. Molloy
Administrative, technical, or material support (i.e., reporting or organizing data, constructing databases): L. Doculara, E. Millar, H.E. Gee, T.J. Molloy
Study supervision: J. Toohey, T.J. Molloy
Other (tissue pathology): E. Millar
Other (histopathology): A. Zaratzian

Acknowledgments

The authors would like to acknowledge funding support from the Cancer Institute New South Wales (11-CDF-3-25; 13/CDF/1-01 to T.J. Molloy, M. Pajic), the Philip Hemstritch Fellowship in Pancreatic Cancer (to M. Pajic), the National Foundation for Medical Research and Innovation (to T.J. Molloy), the National Breast Cancer Foundation (to T.J. Molloy), the Chris O'Brien Lifehouse (to H. Gee, S.A. O'Toole), and the CASS Foundation (to T.J. Molloy). The authors declare no competing financial interests.

The costs of publication of this article were defrayed in part by the payment of page charges. This article must therefore be hereby marked *advertisement* in accordance with 18 U.S.C. Section 1734 solely to indicate this fact.

Received November 23, 2016; revised May 12, 2017; accepted November 2, 2017; published OnlineFirst November 27, 2017.

Downloaded from http://aacrjournals.org/cancerres/article-pdf/78/2/501/2772847/501.pdf by guest on 26 August 2022

References

1. Early Breast Cancer Trialists' Collaborative Group, Darby S, McGale P, Correa C, Taylor C, Arriagada R, et al. Effect of radiotherapy after breast-conserving surgery on 10-year recurrence and 15-year breast cancer death: meta-analysis of individual patient data for 10,801 women in 17 randomised trials. Lancet 2011;378:1707–16.
2. Speers C, Zhao S, Liu M, Bartelink H, Pierce LJ, Feng FY. Development and validation of a novel radiosensitivity signature in human breast cancer. Clin Cancer Res 2015;21:3667–77.
3. Coates AS, Winer EP, Goldhirsch A, Gelber RD, Gnant M, Piccart-Gebhart M, et al. Tailoring therapies–improving the management of early breast cancer: St gallen international expert consensus on the primary therapy of early breast cancer 2015. Ann Oncol 2015;26:1533–46.
4. Gewirtz DA, Hilliker ML, Wilson EN. Promotion of autophagy as a mechanism for radiation sensitization of breast tumor cells. Radiother Oncol 2009;92:323–8.
5. Goldstein M, Kastan MB. The DNA damage response: implications for tumor responses to radiation and chemotherapy. Annu Rev Med 2015;66:129–43.
6. Karar J, Maity A. Modulating the tumor microenvironment to increase radiation responsiveness. Cancer Biol Ther 2009;8:1994–2001.
7. Hong L, Yang Z, Ma J, Fan D. Function of miRNA in controlling drug resistance of human cancers. Curr Drug Targets 2013;14:1118–27.
8. Sun X, Zhang S, Ma X. Prognostic value of MicroRNA-125 in various human malignant neoplasms: a meta-analysis. Clin Lab 2015;61:1667–74.
9. Lanford RE, Hildebrandt-Eriksen ES, Petri A, Persson R, Lindow M, Munk ME, et al. Therapeutic silencing of microRNA-122 in primates with chronic hepatitis C virus infection. Science 2010;327:198–201.
10. Ma W, Ma CN, Zhou NN, Li XD, Zhang YJ. Up- regulation of miR-328-3p sensitizes non-small cell lung cancer to radiotherapy. Sci Rep 2016;6:31651.
11. Hatano K, Kumar B, Zhang Y, Coulter JB, Hedayati M, Mears B, et al. A functional screen identifies miRNAs that inhibit DNA repair and sensitize prostate cancer cells to ionizing radiation. Nucleic Acids Res 2015;43:4075–86.
12. Wang Y, Klijn JG, Zhang Y, Sieuwerts AM, Look MP, Yang F, et al. Gene-expression profiles to predict distant metastasis of lymph-node-negative primary breast cancer. Lancet 2005;365:671–9.
13. Ivshina AV, George J, Senko O, Mow B, Putti TC, Smeds J, et al. Genetic reclassification of histologic grade delineates new clinical subtypes of breast cancer. Cancer Res 2006;66:10292–301.
14. Schmidt M, Bohm D, von Torne C, Steiner E, Puhl A, Pilch H, et al. The humoral immune system has a key prognostic impact in node-negative breast cancer. Cancer Res 2008;68:5405–13.
15. Buffa FM, Camps C, Winchester L, Snell CE, Gee HE, Sheldon H, et al. microRNA-associated progression pathways and potential therapeutic targets identified by integrated mRNA and microRNA expression profiling in breast cancer. Cancer Res 2011;71:5635–45.
16. Nimeus-Malmstrom E, Krogh M, Malmstrom P, Strand C, Fredriksson I, Karlsson P, et al. Gene expression profiling in primary breast cancer distinguishes patients developing local recurrence after breast-conservation surgery, with or without postoperative radiotherapy. Breast Cancer Res 2008;10:R34.
17. Curtis C, Shah SP, Chin SF, Turashvili G, Rueda OM, Dunning MJ, et al. The genomic and transcriptomic architecture of 2,000 breast tumours reveals novel subgroups. Nature 2012;486:346–52.
18. Altman DG, Lausen B, Sauerbrei W, Schumacher M. Dangers of using "optimal" cutpoints in the evaluation of prognostic factors. J Natl Cancer Inst 1994;86:829–35.
19. McShane LM, Altman DG, Sauerbrei W, Taube SE, Gion M, Clark GM, et al. REporting recommendations for tumour MARKer prognostic studies (REMARK). Br J Cancer 2005;93:387–91.
20. Hudis CA, Barlow WE, Costantino JP, Gray RJ, Pritchard KI, Chapman JA, et al. Proposal for standardized definitions for efficacy end points in adjuvant breast cancer trials: the STEEP system. J Clin Oncol 2007;25:2127–32.
21. Millar EK, Graham PH, O'Toole SA, McNeil CM, Browne L, Morey AL, et al. Prediction of local recurrence, distant metastases, and death after breast-conserving therapy in early-stage invasive breast cancer using a five-biomarker panel. J Clin Oncol 2009;27:4701–8.
22. Li JH, Liu S, Zhou H, Qu LH, Yang JH. starBase v2.0: decoding miRNA-ceRNA, miRNA-ncRNA and protein-RNA interaction networks from large-scale CLIP-Seq data. Nucleic Acids Res 2014;42:D92–D7.
23. Yates LA, Norbury CJ, Gilbert RJ. The long and short of microRNA. Cell 2013;153:516–9.
24. Krishnan K, Steptoe AL, Martin HC, Pattabiraman DR, Nones K, Waddell N, et al. miR-139-5p is a regulator of metastatic pathways in breast cancer. RNA 2013;19:1767–80.
25. Miranda KC, Huynh T, Tay Y, Ang YS, Tam WL, Thomson AM, et al. A pattern-based method for the identification of MicroRNA binding sites and their corresponding heteroduplexes. Cell 2006;126:1203–17.
26. Higgins GS, Prevo R, Lee YF, Helleday T, Muschel RJ, Taylor S, et al. A small interfering RNA screen of genes involved in DNA repair identifies tumor-specific radiosensitization by POLQ knockdown. Cancer Res 2010;70:2984–93.

27. Hurov KE, Cotta-Ramusino C, Elledge SJ. A genetic screen identifies the Triple T complex required for DNA damage signaling and ATM and ATR stability. Genes Dev 2010;24:1939–50.
28. Sudo H, Tsuji AB, Sugyo A, Imai T, Saga T, Harada YN. A loss of function screen identifies nine new radiation susceptibility genes. Biochem Biophys Res Commun 2007;364:695–701.
29. Bonner WM, Redon CE, Dickey JS, Nakamura AJ, Sedelnikova OA, Solier S, et al. GammaH2AX and cancer. Nat Rev Cancer 2008;8:957–67.
30. Loeb LA, Preston BD. Mutagenesis by apurinic/apyrimidinic sites. Annu Rev Genet 1986;20:201–30.
31. Roberts SA, Strande N, Burkhalter MD, Strom C, Havener JM, Hasty P, et al. Ku is a 5′-dRP/AP lyase that excises nucleotide damage near broken ends. Nature 2010;464:1214–7.
32. Yoshimura M, Kohzaki M, Nakamura J, Asagoshi K, Sonoda E, Hou E, et al. Vertebrate POLQ and POLbeta cooperate in base excision repair of oxidative DNA damage. Mol Cell 2006;24:115–25.
33. Vazquez-Chantada M, Ariz U, Varela-Rey M, Embade N, Martinez-Lopez N, Fernandez-Ramos D, et al. Evidence for LKB1/AMP-activated protein kinase/endothelial nitric oxide synthase cascade regulated by hepatocyte growth factor, S-adenosylmethionine, and nitric oxide in hepatocyte proliferation. Hepatology 2009;49:608–17.
34. Erdmann K, Cheung BW, Immenschuh S, Schroder H. Heme oxygenase-1 is a novel target and antioxidant mediator of S-adenosylmethionine. Biochem Biophys Res Commun 2008;368:937–41.
35. Bergh J, Norberg T, Sjogren S, Lindgren A, Holmberg L. Complete sequencing of the p53 gene provides prognostic information in breast cancer patients, particularly in relation to adjuvant systemic therapy and radiotherapy. Nat Med 1995;1:1029–34.
36. Kota J, Chivukula RR, O'Donnell KA, Wentzel EA, Montgomery CL, Hwang HW, et al. Therapeutic microRNA delivery suppresses tumorigenesis in a murine liver cancer model. Cell 2009;137:1005–17.
37. Ringborg U, Bergqvist D, Brorsson B, Cavallin-Stahl E, Ceberg J, Einhorn N, et al. The Swedish Council on Technology Assessment in Health Care (SBU) systematic overview of radiotherapy for cancer including a prospective survey of radiotherapy practice in Sweden 2001—summary and conclusions. Acta Oncol 2003;42:357–65.
38. Guo H, Hu X, Ge S, Qian G, Zhang J. Regulation of RAP1B by miR-139 suppresses human colorectal carcinoma cell proliferation. Int J Biochem Cell Biol 2012;44:1465–72.
39. Liu R, Yang M, Meng Y, Liao J, Sheng J, Pu Y, et al. Tumor-suppressive function of miR-139-5p in esophageal squamous cell carcinoma. PLoS One 2013;8:e77068.
40. Mateos-Gomez PA, Gong F, Nair N, Miller KM, Lazzerini-Denchi E, Sfeir A. Mammalian polymerase theta promotes alternative NHEJ and suppresses recombination. Nature 2015;518:254–7.
41. Katsura Y, Sasaki S, Sato M, Yamaoka K, Suzukawa K, Nagasawa T, et al. Involvement of Ku80 in microhomology-mediated end joining for DNA double-strand breaks in vivo. DNA Repair 2007;6:639–48.
42. Higgins GS, Harris AL, Prevo R, Helleday T, McKenna WG, Buffa FM. Overexpression of POLQ confers a poor prognosis in early breast cancer patients. Oncotarget 2010;1:175–84.
43. Mason JM, Dusad K, Wright WD, Grubb J, Budke B, Heyer WD, et al. RAD54 family translocases counter genotoxic effects of RAD51 in human tumor cells. Nucleic Acids Res 2015;43:3180–96.
44. Mao Y, Muller MT. Down modulation of topoisomerase I affects DNA repair efficiency. DNA Repair 2003;2:1115–26.
45. Du Y, Zhou Q, Yin W, Zhou L, Di G, Shen Z, et al. The role of topoisomerase IIalpha in predicting sensitivity to anthracyclines in breast cancer patients: a meta-analysis of published literatures. Breast Cancer Res Treat 2011;129:839–48.
46. Mao Z, Liu S, Cai J, Huang ZZ, Lu SC. Cloning and functional characterization of the 5′-flanking region of human methionine adenosyltransferase 2A gene. Biochem Biophys Res Commun 1998;248:479–84.
47. Croce CM.Causes and consequences of microRNA dysregulation in cancer. Nat Rev Genet 2009;10:704–14.
48. Ceccaldi R, Liu JC, Amunugama R, Hajdu I, Primack B, Petalcorin MI, et al. Homologous-recombination-deficient tumours are dependent on Poltheta-mediated repair. Nature 2015;518:258–62.
49. Gee HE, Buffa FM, Harris AL, Toohey JM, Carroll SL, Cooper CL, et al. MicroRNA-Related DNA repair/cell-cycle genes independently associated with relapse after radiation therapy for early breast cancer. Int J Radiat Oncol Biol Phys 2015;93:1104–14.
50. Di Saverio S, Catena F, Santini D, Ansaloni L, Fogacci T, Mignani S, et al. 259 Patients with DCIS of the breast applying USC/Van Nuys prognostic index: a retrospective review with long term follow up. Breast Cancer Res Treat 2008;109:405–16.
51. Donker M, Litiere S, Werutsky G, Julien JP, Fentiman IS, Agresti R, et al. Breast-conserving treatment with or without radiotherapy in ductal carcinoma In Situ: 15-year recurrence rates and outcome after a recurrence, from the EORTC 10853 randomized phase III trial. J Clin Oncol 2013;31:4054–9.
52. Grantzau T, Mellemkjaer L, Overgaard J. Second primary cancers after adjuvant radiotherapy in early breast cancer patients: a national population based study under the danish breast cancer cooperative group (DBCG). Radiother Oncol 2013;106:42–9.
53. Bader AG.miR-34—a microRNA replacement therapy is headed to the clinic. Front Genet 2012;3:120.
54. Rayner KJ, Esau CC, Hussain FN, McDaniel AL, Marshall SM, van Gils JM, et al. Inhibition of miR-33a/b in non-human primates raises plasma HDL and lowers VLDL triglycerides. Nature 2011;478:404–7.

Downloaded from http://aacrjournals.org/cancerres/article-pdf/78/2/501/2772847/501.pdf by guest on 26 August 2022